Journal of the Optical Society of America A
OPTICS, IMAGE SCIENCE, AND VISION

Electromagnetic energy in multilayered spherical particles

Ilia L. Rasskazov,[1,*] Alexander Moroz,[2] and P. Scott Carney[1]

[1]The Institute of Optics, University of Rochester, Rochester, New York 14627, USA
[2]Wave-scattering.com (e-mail: wavescattering@yahoo.com)
*Corresponding author: irasskaz@ur.rochester.edu

Received 9 May 2019; revised 30 July 2019; accepted 31 July 2019; posted 31 July 2019 (Doc. ID 366620); published 27 August 2019

We obtain exact analytic expressions for (i) the electromagnetic energy radial density within and outside a multilayered sphere and (ii) the total electromagnetic energy stored within its core and each of its shells. Explicit expressions for the special cases of lossless core and shell are also provided. The general solution is based on the compact recursive transfer-matrix method, and its validity includes also magnetic media. The theory is illustrated on examples of electric field enhancement within various metallo–dielectric silica–gold multilayered spheres. The user-friendly MATLAB code, which includes the theoretical treatment, is available as a supplement to the paper.

https://doi.org/10.1364/JOSAA.36.001591

1. INTRODUCTION

Multilayered spherical particles of various sizes and material composition are an important part of modern science and technology due to exceptionally adjustable and extraordinary electromagnetic properties. In this regard, the interaction of the electromagnetic wave with a multilayered spherical particle under plane-wave [1–11] or general beam [12–16] illuminations represents a problem of long-standing interest. The solution of this problem implies the definition of the electromagnetic field within or outside a sphere, which allows one to obtain its absorption, scattering, extinction, or other important characteristics. Among these properties, the cycle- and orientation-averaged electric $|\mathbf{E}|^2$ and magnetic $|\mathbf{H}|^2$ fields (in general, electromagnetic energy) within a particular layer (shell) or in the vicinity of a multilayered sphere are of great importance, since they define performance and suitability of a multilayered sphere for a large number of intriguing applications: nonlinear optics [17–19], lasing [20–22], heating [23–25], photocatalysis [26], fluorescence enhancement [27–30], plasmon-enhanced upconversion [31,32], energy harvesting and storing [33–36], surface-enhanced Raman spectroscopy [37–39], biology, and medicine [40–44].

Thus, specific attention is drawn to theoretical considerations of the electromagnetic energy within and in proximity to multilayered spherical particles. This fundamental problem has been thoroughly studied for homogeneous spheres: exact analytic expressions are reported for the electromagnetic energy in dielectric [45,46], magnetic [47], and chiral [48] spheres. These solutions have been extended for two-layered [20,49] and three-layered [39] spheres by using the recursive relations, which makes corresponding analytic representation quite cumbersome and difficult to generalize for $N > 3$ shells. Alternatively, a semi-analytic approach might be used for estimating orientation-averaged local fields [37], which involves *analytic* representation of electromagnetic field within the spherical particle and its consequent *numeric* integration within the volume of a particle [50]. However, given that various optimization algorithms [51,52] are used to find the optimal design of multilayered spheres for a particular application, the development of closed-form analytic expressions becomes highly desirable. Here, we fulfill this need and present a rigorous and, quite importantly, compact analytic solution for (i) the electromagnetic energy radial density within and outside a multilayered sphere and (ii) the total electromagnetic energy within its core and each of its shells.

The paper is organized as follows. In Section 2, we provide a brief overview of the recursive transfer-matrix solution of the electromagnetic light scattering from a multilayered sphere, which has been proposed and thoroughly discussed in Ref. [27]; in Section 3, within the framework of this formalism, we derive a solution for the electromagnetic energy and its density within the multilayered sphere; in Section 4, we provide explicit expressions for specific cases of the electromagnetic energy stored within a core of a multilayered sphere, in a lossless shell, and in the surrounding medium close to a sphere. Discussion of numerical results for silica–gold multilayered nanospheres is given in Section 5. Finally, we draw conclusive remarks in Section 6 and provide useful relations and derivations in Appendices A–C.

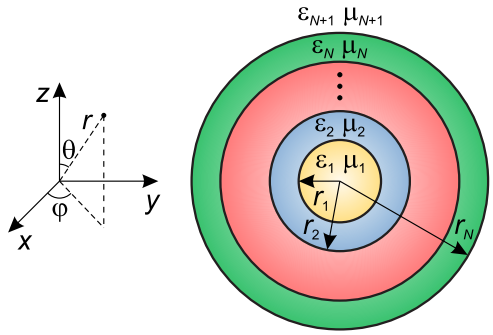

Fig. 1. Schematic representation of the multilayered sphere embedded in a homogeneous isotropic host medium with permittivity $\varepsilon_h = \varepsilon_{N+1}$ and permeability $\mu_h = \mu_{N+1}$. Note that the center of the sphere is located at the origin of the reference system, which is shown separately for convenience.

2. RECURSIVE TRANSFER-MATRIX METHOD

Consider a multilayered sphere with N concentric shells as shown in Fig. 1. The sphere core counts as a shell with number $n = 1$ and the host medium is the $n = N + 1$ shell. Each shell is assumed to be homogeneous and isotropic with scalar permittivity ε_n and permeability μ_n. The outer radius of the n-th shell is denoted by r_n. Spherical coordinates are centered at the sphere origin.

We assume that the multilayered sphere is illuminated with a harmonic electromagnetic wave having vacuum wavelength λ. The corresponding wave vector in the n-th shell is $k_n = \eta_n \omega/c = 2\pi\eta_n/\lambda$, where c is the speed of light in vacuum, ω is frequency, and $\eta_n = \sqrt{\varepsilon_n \mu_n}$ is the refractive index. Electromagnetic fields in any shell are described by the stationary macroscopic Maxwell's equations (in Gaussian units, with time dependence $e^{-i\omega t}$ assumed and suppressed throughout the paper):

$$\mathbf{E} = \frac{ic}{\omega\varepsilon}(\nabla \times \mathbf{H}), \qquad \mathbf{H} = -\frac{ic}{\omega\mu}(\nabla \times \mathbf{E}), \tag{1}$$

where the permittivity ε and permeability μ are scalars.

Following the notation of [27], the basis of normalized (normalization here refers to angular integration) *transverse* vector multipole fields $\nabla \cdot \mathbf{F}_{\gamma L} \equiv 0$ that satisfy the vector Helmholtz equation

$$\nabla \times \left[\nabla \times \mathbf{F}_{\gamma L}(k, \mathbf{r})\right] = k^2 \mathbf{F}_{\gamma L}(k, \mathbf{r})$$

for n-th shell, $1 \le n \le N + 1$, can be formed as [27]

$$\mathbf{F}_{ML}(k_n, \mathbf{r}) = f_{ML}(k_n r)\mathbf{Y}_L^{(m)}(\mathbf{r}),$$

$$\mathbf{F}_{EL}(k_n, \mathbf{r}) = \frac{1}{k_n r}\left\{\sqrt{l(l+1)}\, f_{EL}(k_n r)\mathbf{Y}_L^{(o)}(\mathbf{r}) + \frac{\mathrm{d}}{\mathrm{d}r}\left[r\, f_{EL}(k_n r)\right]\mathbf{Y}_L^{(e)}(\mathbf{r})\right\}, \tag{2}$$

where

$$\tilde{\mathbf{F}}_{EL}(k_n, \mathbf{r}) = \frac{1}{k_n}\nabla \times \mathbf{F}_{ML}(k_n, \mathbf{r}),$$

$$\tilde{\mathbf{F}}_{ML}(k_n, \mathbf{r}) = \frac{1}{k_n}\nabla \times \mathbf{F}_{EL}(k_n, \mathbf{r}), \tag{3}$$

with $\tilde{f}_{EL} = f_{ML}$ and $\tilde{f}_{ML} = f_{EL}$. Here, $L = lm$ is a composite angular momentum index; $\mathbf{Y}_L^{(m)}$, $\mathbf{Y}_L^{(o)}$, and $\mathbf{Y}_L^{(e)}$ are, respectively, magnetic, longitudinal, and electric vector spherical harmonics of degree l and order m (see Appendix A for their definition), and $f_{\gamma L}$ is a suitable linear combination of spherical Bessel functions. Provided that the multipole fields in Eq. (2) represent $\mathbf{E}$, the respective subscripts M and E denote the *magnetic*, or *transverse electric* (TE), and *electric*, or *transverse magnetic* (TM), polarizations, respectively [53].

In the respective cases in which $f_{\gamma l} = j_l$ and $f_{\gamma l} = h_l^{(1)}$, where j_l and $h_l^{(1)}$ are the spherical Bessel functions of the first and third kinds, correspondingly, the multipoles $\mathbf{F}_{\gamma L}$ will be denoted as $\mathbf{J}_{\gamma L}$ and $\mathbf{H}_{\gamma L}$. A general solution for the electric field in the n-th shell, $1 \le n \le N + 1$, reads then as [27]

$$\mathbf{E}_\gamma(\mathbf{r}) = \sum_L \mathbf{F}_{\gamma L}(k_n, \mathbf{r}) = \sum_{\gamma, L}\left[A_{\gamma L}(n)\mathbf{J}_{\gamma L}(k_n, \mathbf{r}) + B_{\gamma L}(n)\mathbf{H}_{\gamma L}(k_n, \mathbf{r})\right],$$

with corresponding

$$f_{\gamma L} = A_{\gamma L}(n)\, j_l(k_n r) + B_{\gamma L}(n) h_l^{(1)}(k_n r) \tag{4}$$

to be determined. The expansion of magnetic field $\mathbf{H}$ is related to that of the electric field $\mathbf{E}$ by the stationary macroscopic Maxwell's equations (1) on using relations (3).

Expansion coefficients $A_{\gamma L}(n)$ and $B_{\gamma L}(n)$ are determined by matching fields across the shell interfaces, i.e., requiring that the tangential components of $\mathbf{E}$ and $\mathbf{H}$ are continuous. For the surrounding medium, i.e., the $(N+1)$-th shell, the expansion coefficients will occasionally be written as

$$C_{\gamma L} \equiv A_{\gamma L}(N+1), \qquad D_{\gamma L} \equiv B_{\gamma L}(N+1).$$

Coefficients $A_{\gamma L}(n)$ and $B_{\gamma L}(n)$ can be found via the transfer-matrix solution in terms of 2×2 *lowering* (backward) $T_{\gamma l}^{-}(n)$ and *raising* (forward) $T_{\gamma l}^{+}(n)$ transfer matrices [27]. The *raising* transfer matrices translate the expansion coefficients $A_{\gamma L}(n)$ and $B_{\gamma L}(n)$ from the n-th shell into the coefficients $A_{\gamma L}(n+1)$ and $B_{\gamma L}(n+1)$ in the $(n+1)$-th shell:

$$\begin{pmatrix} A_{\gamma L}(n+1) \\ B_{\gamma L}(n+1) \end{pmatrix} = T_{\gamma l}^{+}(n) \begin{pmatrix} A_{\gamma L}(n) \\ B_{\gamma L}(n) \end{pmatrix}, \tag{5}$$

whereas the *lowering* transfer matrices translate the coefficients $A(n+1)$ and $B(n+1)$ in the $(n+1)$-th shell into the coefficients $A(n)$ and $B(n)$ in the n-th shell:

$$\begin{pmatrix} A_{\gamma L}(n) \\ B_{\gamma L}(n) \end{pmatrix} = T_{\gamma l}^{-}(n) \begin{pmatrix} A_{\gamma L}(n+1) \\ B_{\gamma L}(n+1) \end{pmatrix}. \tag{6}$$

It can be easily seen from Eqs. (5) and (6) that the *lowering* and *raising* transfer matrices are related as

$$[T_{\gamma l}^{+}(n)]^{-1} = T_{\gamma l}^{-}(n), \qquad [T_{\gamma l}^{-}(n)]^{-1} = T_{\gamma l}^{+}(n). \tag{7}$$

Provided that the coefficients $A_{\gamma L}(n+1)$ and $B_{\gamma L}(n+1)$ are known, the coefficients $A_{\gamma L}(n)$ and $B_{\gamma L}(n)$ can be unambiguously determined, and vice versa. The constituent transfer matrices $T_{\gamma l}^{+}$ and $T_{\gamma l}^{-}$ can be viewed as analogous to *ladder* operators of quantum mechanics.

To determine the expansion coefficients at any shell, *mixed* boundary conditions are imposed, which fix *two* of the coefficients $A_{\gamma L}(n)$ and $B_{\gamma L}(n')$ for each given γ and L, where in general, $n \neq n'$:

1. the *regularity* condition of the solution at the sphere origin, which eliminates $h_l^{(1)}(0) \to \infty$ for $f_{\gamma l}$ in Eq. (4):
$$B_{EL}(1) = B_{ML}(1) \equiv 0; \tag{8}$$
2. for a given frequency ω, the $A_{\gamma L}(N+1) = C_{\gamma L}$ coefficients are equal to the expansion coefficients of an incident electromagnetic field in spherical coordinates.

For general (e.g., focused or Gaussian) beams, numerical integration is, as a rule, required to arrive at the expansion coefficients [12,13,15,16]. Nevertheless, closed analytic expressions for the $C_{\gamma L} = 0$'s are known for two important incident fields. The most familiar example, which we shall examine in detail below, is furnished by incident plane electromagnetic wave $\mathbf{E}(\mathbf{r}) = \mathbf{E}_0 \exp(i\mathbf{k}\cdot\mathbf{r})$, whose expansion in vector spherical wave functions reads as

$$\mathbf{E}_0 \exp(i\mathbf{k}\cdot\mathbf{r}) = \sum_L C_{\gamma L}\mathbf{J}_{\gamma L}(kr), \tag{9}$$

where

$$C_{ML} = 4\pi i^l \mathbf{E}_0 \cdot \mathbf{Y}_L^{(m)*}(\mathbf{k}), \quad C_{EL} = 4\pi i^{l-1}\mathbf{E}_0 \cdot \mathbf{Y}_L^{(e)*}(\mathbf{k}), \tag{10}$$

and the asterisk denotes a complex conjugate. In particular, for the plane wave incident along the z axis and polarized along the x axis (i.e., parallel to $\hat{\mathbf{e}}_\vartheta$ for $\varphi = 0$),

$$C_{ML} = i^l\sqrt{(2l+1)\pi}\,E_0\,\delta_{m,\pm1},$$
$$C_{EL} = \pm i^l\sqrt{(2l+1)\pi}\,E_0\,\delta_{m,\pm1},$$

where $\delta_{mm'}$ is the Kronecker delta function. For an incident dipole field, see Ref. [27].

Irrespective of the incident field, one has the following explicit expressions for the constituent *backward* and *forward* transfer matrices [27]:

$$T_{Ml}^{-}(n) = -i\begin{pmatrix} \tilde\eta\zeta_l'(x)\psi_l(\tilde x) - \tilde\mu\zeta_l(x)\psi_l'(\tilde x) & \tilde\eta\zeta_l'(x)\zeta_l(\tilde x) - \tilde\mu\zeta_l(x)\zeta_l'(\tilde x) \\ -\tilde\eta\psi_l'(x)\psi_l(\tilde x) + \tilde\mu\psi_l(x)\psi_l'(\tilde x) & -\tilde\eta\psi_l'(x)\zeta_l(\tilde x) + \tilde\mu\psi_l(x)\zeta_l'(\tilde x)\end{pmatrix}, \tag{11}$$

$$T_{El}^{-}(n) = -i\begin{pmatrix} \tilde\mu\zeta_l'(x)\psi_l(\tilde x) - \tilde\eta\zeta_l(x)\psi_l'(\tilde x) & \tilde\mu\zeta_l'(x)\zeta_l(\tilde x) - \tilde\eta\zeta_l(x)\zeta_l'(\tilde x) \\ -\tilde\mu\psi_l'(x)\psi_l(\tilde x) + \tilde\eta\psi_l(x)\psi_l'(\tilde x) & -\tilde\mu\psi_l'(x)\zeta_l(\tilde x) + \tilde\eta\psi_l(x)\zeta_l'(\tilde x)\end{pmatrix}, \tag{12}$$

$$T_{Ml}^{+}(n) = -i\begin{pmatrix} \zeta_l'(\tilde x)\psi_l(x)/\tilde\eta - \zeta_l(\tilde x)\psi_l'(x)/\tilde\mu & \zeta_l'(\tilde x)\zeta_l(x)/\tilde\eta - \zeta_l(\tilde x)\zeta_l'(x)/\tilde\mu \\ -\psi_l'(\tilde x)\psi_l(x)/\tilde\eta + \psi_l(\tilde x)\psi_l'(x)/\tilde\mu & -\psi_l'(\tilde x)\zeta_l(x)/\tilde\eta + \psi_l(\tilde x)\zeta_l'(x)/\tilde\mu\end{pmatrix}, \tag{13}$$

$$T_{El}^{+}(n) = -i\begin{pmatrix} \zeta_l'(\tilde x)\psi_l(x)/\tilde\mu - \zeta_l(\tilde x)\psi_l'(x)/\tilde\eta & \zeta_l'(\tilde x)\zeta_l(x)/\tilde\mu - \zeta_l(\tilde x)\zeta_l'(x)/\tilde\eta \\ -\psi_l'(\tilde x)\psi_l(x)/\tilde\mu + \psi_l(\tilde x)\psi_l'(x)/\tilde\eta & -\psi_l'(\tilde x)\zeta_l(x)/\tilde\mu + \psi_l(\tilde x)\zeta_l'(x)/\tilde\eta\end{pmatrix}, \tag{14}$$

where $\psi_l(x) = x\,j_l(x)$ and $\zeta_l(x) = x\,h_l^{(1)}(x)$ are the Riccati–Bessel functions, prime denotes the derivative with respect to the argument in parentheses, and

$$x_n = k_n r_n, \quad \tilde\eta_n = \eta_n/\eta_{n+1}, \quad \tilde x_n = x_n/\tilde\eta_n, \quad \tilde\mu_n = \mu_n/\mu_{n+1}.$$

For the sake of clarity, the n-subscript has been suppressed in Eqs. (11)–(14). The above relations for $T_{\gamma l}^{-}(n)$ and $T_{\gamma l}^{+}(n)$ are general and valid for any homogeneous and isotropic medium, including *magnetic* materials with $\mu_n \neq 1$.

It occurs that the formalism becomes compact if one introduces the composite transfer matrices $\mathcal{T}_{\gamma l}(n)$ and $\mathcal{M}_{\gamma l}(n)$ defined as ordered (from the left to the right) products of the constituent *forward* and *backward* 2×2 matrices:

$$\mathcal{T}_{\gamma l}(n) = \prod_{j=n-1}^{1} T_{\gamma l}^{+}(j), \qquad \mathcal{M}_{\gamma l}(n) = \prod_{j=n}^{N} T_{\gamma l}^{-}(j).$$

Composite matrices $\mathcal{T}_{\gamma l}(n)$ and $\mathcal{M}_{\gamma l}(n)$ transfer expansion coefficients from the sphere core to the n-th shell, and from the surrounding medium to the n-th shell, respectively. Note that $\mathcal{T}_{\gamma l}(n)$ is defined for $2 \le n \le N+1$, while $\mathcal{M}_{\gamma l}(n)$ is defined for $1 \le n \le N$. Analogous to Eq. (7), the following relations can be applied:

$$[\mathcal{T}_{\gamma l}(N+1)]^{-1} = \mathcal{M}_{\gamma l}(1), \quad [\mathcal{M}_{\gamma l}(1)]^{-1} = \mathcal{T}_{\gamma l}(N+1). \tag{15}$$

Note that the *regularity* condition given by Eq. (8), unambiguously determines the m-independent ratio $D_{\gamma L}/C_{\gamma L}$ [53]:

$$D_{\gamma L}/C_{\gamma L} = \mathcal{T}_{21;\gamma l}(N+1)/\mathcal{T}_{11;\gamma l}(N+1). \tag{16}$$

Here, $\mathcal{T}_{ij;\gamma l}(n)$ denotes the (i,j)-th element of the 2×2 matrix $\mathcal{T}_{\gamma l}(n)$.

Thus far, the electromagnetic field anywhere inside and outside a multilayered sphere is unambiguously determined from a pair of expansion coefficients $A(n)$ and $B(n)$ for the respective n-th shell (including the host medium denoted as $(N+1)$-th shell).

3. ENERGY WITHIN A MULTILAYERED SPHERE

The energy here will have the usual meaning of instant power integrated over a cycle of harmonic excitation [54–57]. The *total* electromagnetic energy W within the multilayered sphere can be obtained by integrating the electromagnetic energy radial density $w_n(r)$ within each n-th shell and, consequently, summing up the total electromagnetic energies W_n stored in each n-th shell:

$$W = \sum_{n=1}^{N} W_n = \sum_{n=1}^{N}\int_{r_{n-1}}^{r_n} w_n(r) r^2 \mathrm{d}r, \tag{17}$$

where $r_0 = 0$ for the core, and

$$w_n(r) = \frac{1}{4}\oint \left[G_e\,(\varepsilon_n)\,|\mathbf{E}(\mathbf{r})|^2 + G_m\,(\mu_n)\,|\mathbf{H}(\mathbf{r})|^2\right] \mathrm{d}\Omega\,. \tag{18}$$

Here, $G_e(\varepsilon_n) = \mathrm{Re}(\varepsilon_n)$ and $G_m(\mu_n) = \mathrm{Re}(\mu_n)$ in the non-dispersive case [46]. For dispersive and absorbing metallic shells, G_m remains the same, while G_e can be described by Loudon's formula [54]: $G_e = [\mathrm{Re}(\varepsilon_n) + 2\omega \mathrm{Im}(\varepsilon_n)/\Gamma_n]$, with Γ_n being the free electron damping constant in the Drude formula.

Angular integration of $|\mathbf{E}|^2$ and $|\mathbf{H}|^2$ in Eq. (18) in any shell can be performed as follows (see Appendix B for details):

$$\oint |\mathbf{E}|^2 \mathrm{d}\Omega = \sum_{l=1}^{\infty}\sum_{m=-l}^{l}\left[|f_{Mlm}|^2 + \frac{l+1}{2l+1}|f_{E,l-1,m}|^2 + \frac{l}{2l+1}|f_{E,l+1,m}|^2\right], \tag{19}$$

$$\oint |\mathbf{H}|^2 \mathrm{d}\Omega = \frac{|\varepsilon_n|}{|\mu_n|}\sum_{l=1}^{\infty}\sum_{m=-l}^{l}\left[|f_{Elm}|^2 + \frac{l+1}{2l+1}|f_{M,l-1,m}|^2 + \frac{l}{2l+1}|f_{M,l+1,m}|^2\right]. \tag{20}$$

The spherical Bessel functions of the order $l \pm 1$ here originate from eliminating the radial derivation in $\mathbf{F}_{EL}$ of Eq. (2) by the identity (B2) in Appendix B.

Below we present exact analytic expressions for each of the above quantities, i.e., $w_n(r)$, W_n, and W. There are two important steps. The first is the summation over m in Eqs. (19) and (20), which we perform by (i) factorizing $f_{\gamma L}$, and then (ii) using sum rules for $C_{\gamma L}$. The second is a radial integration in Eq. (17), which we implement by using Lommel's integration formulas in Appendix C.

A. Factorization of Expansion Coefficients

Expansion coefficients $A_{\gamma L}(n)$ and $B_{\gamma L}(n)$ can be reformulated via forward $\mathcal{T}_{\gamma l}(n)$ and backward $\mathcal{M}_{\gamma l}(n)$ composite transfer matrices as follows:

$$A_{\gamma L}(n) = \mathcal{M}_{11;\gamma l}(n) C_{\gamma L} + \mathcal{M}_{12;\gamma l}(n) D_{\gamma L} = C_{\gamma L}\left[\mathcal{M}_{11;\gamma l}(n) + \mathcal{M}_{12;\gamma l}(n)\frac{\mathcal{T}_{21;\gamma l}(N+1)}{\mathcal{T}_{11;\gamma l}(N+1)}\right], \tag{21}$$

$$B_{\gamma L}(n) = \mathcal{M}_{21;\gamma l}(n) C_{\gamma L} + \mathcal{M}_{22;\gamma l}(n) D_{\gamma L} = C_{\gamma L}\left[\mathcal{M}_{21;\gamma l}(n) + \mathcal{M}_{22;\gamma l}(n)\frac{\mathcal{T}_{21;\gamma l}(N+1)}{\mathcal{T}_{11;\gamma l}(N+1)}\right]. \tag{22}$$

Note that in this representation, coefficients $A_{\gamma L}$ and $B_{\gamma L}$ are products of m-dependent $C_{\gamma L}$ and m-independent expression in square brackets. Due to the linearity of the equations and spherical symmetry of the problem (the latter being reflected in *m-independent* transfer matrix elements), each of the expansion coefficients $A_{\gamma L}$ and $B_{\gamma L}$ can be factorized as a product of a *m-dependent* factor resulting from m-dependence of the expansion coefficients $C_{\gamma L}$, and a *m-independent* factor coming from the transfer matrices:

$$A_{\gamma L}(n) = C_{\gamma L}\bar{A}_{\gamma l}(n), \qquad B_{\gamma L}(n) = C_{\gamma L}\bar{B}_{\gamma l}(n).$$

Hence, each $f_{\gamma L}$ factorizes as

$$f_{\gamma L} = C_{\gamma L}\bar{f}_{\gamma l}, \tag{23}$$

where *m-independent* $\bar{f}_{\gamma l}$ is explicitly defined as

$$\bar{f}_{\gamma l} = \bar{A}_{\gamma l}(n)\, j_l(k_n r) + \bar{B}_{\gamma l}(n) h_l^{(1)}(k_n r). \tag{24}$$

Note that in Eqs. (19) and (20), one has to consider the radial solutions as indexed by γ, l, and $l \pm 1$:

$$\bar{f}_{\gamma l\pm1}(n) = \bar{A}_{\gamma l}(n)\, j_{l\pm1}(k_n r) + \bar{B}_{\gamma l}(n) h_{l\pm1}^{(1)}(k_n r). \tag{25}$$

Since the spherical Bessel functions of the order $l \pm 1$ in Eqs. (19) and (20) originate from eliminating the radial derivation in $\mathbf{F}_{EL}$ of Eq. (2) according to the identity (B2) in Appendix B, they are multiplied by the expansions coefficients $\bar{A}_{\gamma l}$ and $\bar{B}_{\gamma l}$ carrying the index l.

After the factorization given by Eq. (23), integral in Eq. (19) reads as

$$\oint |\mathbf{E}|^2\,\mathrm{d}\Omega = \sum_{l=1}\left[|\bar{f}_{Ml}|^2\sum_{m=-l}^{l}|C_{Mlm}|^2 + \left(\frac{l+1}{2l+1}|\bar{f}_{E,l-1}|^2 + \frac{l}{2l+1}|\bar{f}_{E,l+1}|^2\right)\sum_{m=-l}^{l}|C_{Elm}|^2\right]. \tag{26}$$

Note that Eq. (20) is factorized in a similar manner.

B. Sum Rules

One can eliminate the m-dependence in Eq. (26) recalling Eq. (10) for $C_{\gamma lm}$ and using the sum rules [58,59] for magnetic $\mathbf{Y}_L^{(m)}(\mathrm{r})$ and electric $\mathbf{Y}_L^{(e)}(\mathrm{r})$ vector spherical harmonics:

$$\sum_{m=-l}^{l}\mathbf{Y}_L(\mathrm{r})\otimes\mathbf{Y}_L^*(\mathrm{r}) = \frac{2l+1}{8\pi}\left(\hat{\mathbf{e}}_\vartheta\otimes\hat{\mathbf{e}}_\vartheta + \hat{\mathbf{e}}_\varphi\otimes\hat{\mathbf{e}}_\varphi\right),$$

where $\otimes$ denotes the tensor product. Thus, for plane-wave incidence, the m-dependence in Eq. (26) yields

$$\sum_{m=-l}^{l}|\mathbf{E_0}\cdot\mathbf{Y}_L^{(m,e)*}|^2 = \frac{2l+1}{8\pi}\left(|\mathbf{E}_\theta|^2 + |\mathbf{E}_\phi|^2\right) = \frac{2l+1}{8\pi}|E_0|^2,$$

which is also applicable to a factorized representation of Eq. (20). For an incident dipole field, see Ref. [27].

C. Electromagnetic Energy Radial Density

After the factorization of Eqs. (19) and (20), and subsequent summation over the magnetic number m, we end up with

expressions for the electric,

$$\oint |\mathbf{E}|^2 \mathrm{d}\Omega = 2\pi |E_0|^2 \times \sum_{l=1}^{\infty} [(2l+1)|\bar{f}_{Ml}|^2 + (l+1)|\bar{f}_{E,l-1}|^2 + l|\bar{f}_{E,l+1}|^2], \tag{27}$$

and magnetic,

$$\oint |\mathbf{H}|^2 \mathrm{d}\Omega = 2\pi |E_0|^2 \frac{|\varepsilon_n|}{|\mu_n|} \times \sum_{l=1}^{\infty} [(2l+1)|\bar{f}_{El}|^2 + (l+1)|\bar{f}_{M,l-1}|^2 + l|\bar{f}_{M,l+1}|^2], \tag{28}$$

components of the electromagnetic field.

Thus, the electromagnetic energy radial density in Eq. (18) is explicitly defined with analytic expressions in Eqs. (27) and (28).

D. Total Electromagnetic Energy

Finally, the radial integration of Eqs. (27) and (28) in Eq. (17) can be performed by using Lommel's integration formulas (see Appendix C for details):

$$\int_{r_{n-1}}^{r_n} r^2 \mathrm{d}r \oint |\mathbf{E}|^2 \mathrm{d}\Omega = 2\pi |E_0|^2 \frac{r^3}{x^2 - x^{*2}} \times \sum_{l=1}^{\infty} [(2l+1)\bar{F}_{Ml} + (l+1)\bar{F}_{E,l-1} + l\bar{F}_{E,l+1}] \Big|_{r=r_{n-1}}^{r=r_n}, \tag{29}$$

$$\int_{r_{n-1}}^{r_n} r^2 \mathrm{d}r \oint |\mathbf{H}|^2 \mathrm{d}\Omega = 2\pi |E_0|^2 \frac{r^3}{x^2 - x^{*2}} \frac{|\varepsilon_n|}{|\mu_n|} \times \sum_{l=1}^{\infty} [(2l+1)\bar{F}_{El} + (l+1)\bar{F}_{M,l-1} + l\bar{F}_{M,l+1}] \Big|_{r=r_{n-1}}^{r=r_n}. \tag{30}$$

Here, $x = k_n r$, and purely *imaginary* functions

$$\bar{F}_{\gamma l} = x\bar{f}_{\gamma,l+1}(x)\bar{f}^*_{\gamma l}(x) - x^*\bar{f}_{\gamma l}(x)\bar{f}^*_{\gamma,l+1}(x) = 2i\mathrm{Im}[x\bar{f}_{\gamma,l+1}(x)\bar{f}^*_{\gamma l}(x)] \tag{31}$$

are cancelled by purely *imaginary* $x^2 - x^{*2} = 4i\mathrm{Re}(x)\mathrm{Im}(x)$ in the denominator, which results in purely *real* integrals in Eqs. (29) and (30).

Substitution of Eqs. (29) and (30) into Eqs. (17) and (18) yields an explicit expression for the total electromagnetic energy W_n stored within each shell of the multilayered sphere. The above relations are general and valid within any shell including $(N+1)$-th layer being a surrounding medium.

E. Normalized Electromagnetic Energy

In some cases, it is of practical use to estimate *normalized* electromagnetic energy instead of its absolute value. For example, the electromagnetic energy enhancement determines the performance of the spherical particle in surface-enhanced Raman spectroscopy [37,39] and plasmon-enhanced upconversion [32], and might be important in other cases [60–62]. To obtain the corresponding enhancement factor, one could compare the energy stored within the n-th layer compared to the energy stored in a lossless host medium of the same volume. Given that in a homogeneous medium, $|\mathbf{H}|^2 = (|\varepsilon_h|/|\mu_h|)|\mathbf{E}|^2$, the angularly integrated electromagnetic energy density (18) of the incident wave reduces in the *lossless* host medium to

$$w_0 = w_0^{(e)} + w_0^{(m)} = 2\pi |E_0|^2 \varepsilon_h, \qquad w_0^{(e,m)} = \pi |E_0|^2 \varepsilon_h,$$

where $w_0^{(e)}$ and $w_0^{(m)}$ represent electric and magnetic components of the w_0, respectively. These quantities can be used to normalize the electromagnetic energy radial density $w_n(r)$ in the presence of a general multilayered sphere at the radial distance r from the sphere origin.

On using Eq. (17), the *total* electromagnetic energy stored within the shell with thickness $(r_n - r_{n-1})$ characterized by a *lossless* ε_h, is defined as

$$W_{0n} = \frac{2}{3}\pi |E_0|^2 (r_n^3 - r_{n-1}^3)\varepsilon_h.$$

This quantity can be used to normalize the *total* electromagnetic energy W_n stored within n-th shell.

F. Convergence Criterion

For the completeness of the developed theory, it is insightful to provide general remarks on the summation over l in Eqs. (27)–(30). Numerical implementation of these equations requires the truncation to some finite number $l_{\max}$, which can be defined for a particular value of the size parameter $x = kr$ with a widely used Wiscombe criterion [63]:

$$l_{\max} = \begin{cases} x + 4x^{1/3} + 1, & 0.02 \le x \le 8 \\ x + 4.05x^{1/3} + 2, & 8 < x < 4200 \\ x + 4x^{1/3} + 2, & 4200 < x < 20000. \end{cases}$$

However, this criterion may vary for near and far fields [64].

For large values of the size parameter, one could face convergence issues, because the theoretical treatment for multilayered spherical particles inevitably involves calculation of the difference of the products of the Riccati–Bessel functions. The most successful way to mitigate these issues is to factorize Riccati–Bessel functions with their logarithmic derivatives as shown in Ref. [8].

4. SPECIAL CASES

Although presented formalism is rigorous and valid for a general multilayered sphere, it is insightful to discuss some special cases and provide corresponding explicit expressions, which might be handier to use.

A. Core Region

For the core region, with $n=1$, Eq. (21) reduces on using Eq. (15) to

$$A_{\gamma L}(1)=\frac{C_{\gamma L}}{\mathcal{T}_{11;\gamma l}(N+1)}. \tag{32}$$

Note that $B_{\gamma L}=0$ due to the regularity condition given in Eq. (8). Thus, on using Eq. (32) and Eqs. (23)–(25),

$$\bar{f}_{\gamma l}=\frac{j_l(k_1 r)}{\mathcal{T}_{11;\gamma l}(N+1)},\qquad \bar{f}_{\gamma l\pm1}=\frac{j_{l\pm1}(k_1 r)}{\mathcal{T}_{11;\gamma l}(N+1)}. \tag{33}$$

We emphasize that $\bar{f}_{\gamma l}$ and $\bar{f}_{\gamma l\pm1}$ have the same denominator according to Eqs. (24) and (25).

Thus, the *total* electromagnetic energy stored inside a core of a general multilayered sphere extending from $r=0$ to $r=r_1$ reads as

$$W_1=\int_0^{r_1} w_1(r)r^2\mathrm{d}r=\frac{\pi|E_0|^2}{2}\frac{r_1^3}{x_1^2-x_1^{*2}}$$
$$\times\sum_{l=1}^{\infty}\left\{(2l+1)\bar{F}_l^{(1)}\left[\frac{G_e(\varepsilon_1)}{|\mathcal{T}_{11;Ml}(N+1)|^2}+\frac{|\varepsilon_1|}{|\mu_1|}\frac{G_m(\mu_1)}{|\mathcal{T}_{11;El}(N+1)|^2}\right]\right.$$
$$+(l+1)\bar{F}_{l-1}^{(1)}\left[\frac{G_e(\varepsilon_1)}{|\mathcal{T}_{11;El}(N+1)|^2}+\frac{|\varepsilon_1|}{|\mu_1|}\frac{G_m(\mu_1)}{|\mathcal{T}_{11;Ml}(N+1)|^2}\right]$$
$$\left.+l\bar{F}_{l+1}^{(1)}\left[\frac{G_e(\varepsilon_1)}{|\mathcal{T}_{11;El}(N+1)|^2}+\frac{|\varepsilon_1|}{|\mu_1|}\frac{G_m(\mu_1)}{|\mathcal{T}_{11;Ml}(N+1)|^2}\right]\right\}, \tag{34}$$

where $\bar{F}_l^{(1)}=2i\mathrm{Im}[x_1 j_{l+1}(x_1)j_l^*(x_1)]$.

Known results for the electromagnetic energy within a nonmagnetic [46] and magnetic [47] homogeneous sphere can be recovered from Eq. (34) by considering the special case of $N=1$.

B. Lossless Shell

The lossless shell case can be obtained by taking the limit $\mathrm{Im}(\eta)\to0$, which yields in $x=x^*$, and, as a consequence, vanishing of the denominator in Eqs. (29) and (30). After applying l'Hôpital's rule (see Appendix C for details), Eqs. (29) and (30) read as

$$\int_{r_{n-1}}^{r_n} r^2\mathrm{d}r\oint|\mathbf{E}|^2\mathrm{d}\Omega=\pi|E_0|^2\frac{r^3}{x}$$
$$\times\sum_{l=1}^{\infty}[(2l+1)\bar{\Lambda}_{Ml}+(l+1)\bar{\Lambda}_{E,l-1}+l\bar{\Lambda}_{E,l+1}]\Big|_{r=r_{n-1}}^{r=r_n}, \tag{35}$$

$$\int_{r_{n-1}}^{r_n} r^2\mathrm{d}r\oint|\mathbf{H}|^2\mathrm{d}\Omega=\pi|E_0|^2\frac{r^3}{x}\frac{|\varepsilon_n|}{|\mu_n|}$$
$$\times\sum_{l=1}^{\infty}[(2l+1)\bar{\Lambda}_{El}+(l+1)\bar{\Lambda}_{M,l-1}+l\bar{\Lambda}_{M,l+1}]\Big|_{r=r_{n-1}}^{r=r_n}, \tag{36}$$

where $r_0=0$, and m-independent parameter

$$\bar{\Lambda}_{\gamma l}=x(|\bar{f}_{\gamma l}|^2+|\bar{f}_{\gamma l+1}|^2)-(2l+1)\mathrm{Re}(\bar{f}_{\gamma l}\bar{f}_{\gamma l+1}^*). \tag{37}$$

Of note, Eqs. (35)–(37) are also valid for a lossless core, although appropriate expressions for $\bar{f}_{\gamma l}$ and $\bar{f}_{\gamma l+1}$ from Eq. (33) have to be used.

C. Electromagnetic Field in the Vicinity of a Sphere

Finally, for many applications, it is of interest to get the angular averaged electric or magnetic field intensity outside a multilayered particle. Assuming the plane-wave incidence and the corresponding plane-wave expansion in vector spherical wave functions given by Eq. (9), the electric field outside a spherical particle is defined as

$$\mathbf{E}(\mathbf{r})=\sum_{\gamma,L}\left[C_{\gamma L}\mathbf{J}_{\gamma L}(k_h,\mathbf{r})+D_{\gamma L}\mathbf{H}_{\gamma L}(k_h,\mathbf{r})\right]$$
$$=\sum_{L}\mathbf{F}_{\gamma L}(k_n,\mathbf{r})=\sum_{L}C_{\gamma L}\bar{\mathbf{F}}_{\gamma L}(k_h,\mathbf{r}), \tag{38}$$

where $f_{\gamma L}$ in $\mathbf{F}_{\gamma L}$ are given by [27]

$$f_{\gamma L}=C_{\gamma L}j_l(k_n r)+D_{\gamma L}h_l^{(1)}(k_n r)$$
$$=C_{\gamma L}\left[j_l(k_h r)+h_l(k_h r)\frac{\mathcal{T}_{21;\gamma l}(N+1)}{\mathcal{T}_{11;\gamma l}(N+1)}\right]=C_{\gamma L}\bar{f}_{\gamma l}. \tag{39}$$

Here, the *m-dependent* coefficients $C_{\gamma L}$ are given by Eqs. (10) and (16), for *m-independent* ratio $D_{\gamma L}/C_{\gamma L}$ has been used.

One can now proceed as before when arriving at Eq. (27) to yield formally in the same formula, but with $\bar{f}_{\gamma l}$ given in Eq. (39). Corresponding enhancement of the average electric field intensity at the distance $r>r_N$ from the center of a spherical particle can be obtained after normalization Eq. (27) to $4\pi|E_0|^2$. The magnetic field enhancement near a multilayered sphere can be obtained analogously.

5. DISCUSSION

For the sake of illustration, we apply theory developed here to metallo–dielectric multilayered nanospheres. Appropriately designed by well-developed fabrication procedures [65,66], such nanoparticles attract significant attention since they may extraordinarily absorb [67–69], scatter [70], or transmit [71–73] electromagnetic irradiation, and serve as a platform for photonic bandgap structures [74–77] or hyperbolic media [78].

Figure 2 shows the normalized electric energy radial density $w_n^{(e)}(r)/w_0^{(e)}$ [which corresponds to the normalized electric term in Eq. (18)] for widely used silica–gold nanospheres. $w_n^{(e)}(r)/w_0^{(e)}$ is shown for a number of SiO_2–Au spheres of different compositions, consisting of $n=1$, 2, 3, 5 or seven layers with varying thicknesses. It can be seen that our theory makes it convenient to investigate the electromagnetic field localization within the multilayered spheres. In a particular case of our study, one can observe wavelength-dependent features of the electric field localization within the various layers, depending on the particle composition: $w_n^{(e)}(r)/w_0^{(e)}$ acquires maximum values at different λ, from visible to near-IR, and within different

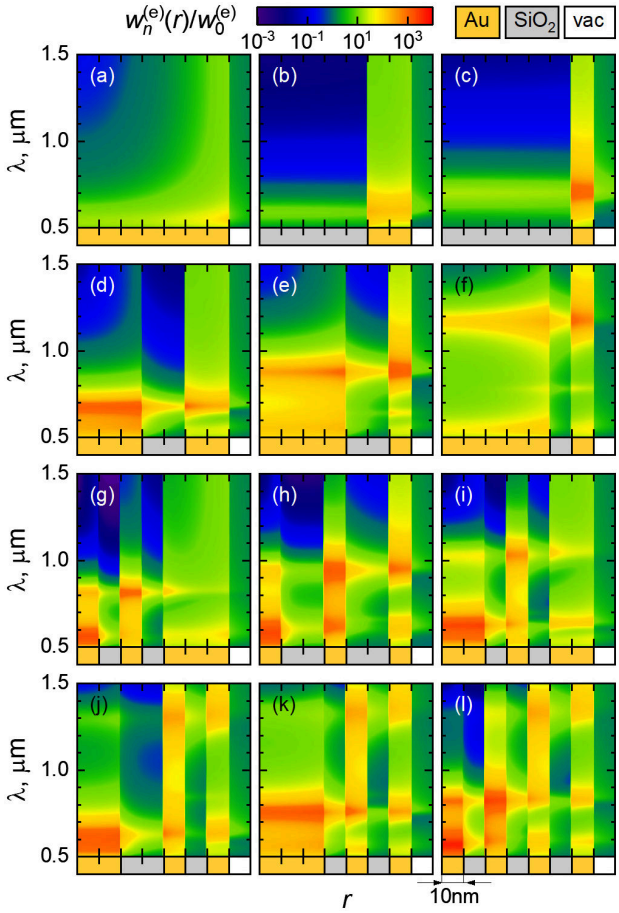

Fig. 2. Normalized *electric* energy radial density within and in the vicinity of the multilayered SiO_2-Au spherical particles of fixed radius $r_N = 70$ nm embedded in a vacuum with $\varepsilon_b = \mu_b = 1$. Refractive index of SiO_2 is assumed to be 1.45, while the experimental data from Ref. [79] have been used for the refractive index of Au, with the electron mean free path correction [80,81] for thin shells. Loudon's formula [54] for G_e has been employed with corresponding data for Drude model of Au [82]. Different spheres composition, as denoted with colored bars on the bottom of each plot, with the rightmost 10 nm corresponding to the surrounding vacuum, have been considered: (a) solid Au sphere; (b), (c) SiO_2/Au; (d)–(f) Au/SiO_2/Au; (g)–(k) Au/SiO_2/Au/SiO_2/Au; and (l) Au/SiO_2/Au/SiO_2/Au/SiO_2/Au multilayered spheres.

layers. Taking as a benchmark the immediate exterior of a homogeneous Au sphere, significant energy density enhancements can be observed both inside and outside the multilayered particles.

6. CONCLUSION

We have presented a self-consistent rigorous theory for the electromagnetic energy within a general multilayered sphere, which is applicable to general illumination. Our main focus was on plane-wave illumination for which we obtained exact analytic expressions for (i) the electromagnetic energy radial density within and outside a multilayered sphere and (ii) the total electromagnetic energy stored within its core and each of its shells. Other types of excitation [12,13,15,16,27,83–85] require substitution of corresponding expressions of expansion coefficients $C_{\gamma L}$ for those in Eq. (10).

The reported formalism is valid for a wide range of sphere sizes and materials, including magnetic materials. Multilayered spheres from anisotropic [86,87] or chiral [48] materials can also be considered with the presented formalism after modification. We emphasize that known explicit expressions for homogeneous [46,47] or core-shell [49,88] spherical particles can be easily obtained on using our general formalism for a special case of $N = 1$ or $N = 2$, correspondingly.

The theory developed here could have numerous applications. The most straightforward are heating and nonlinear optics applications, which require the determination of $|\mathbf{E}|^2$ or its higher powers. Although only the electric part of electromagnetic energy has been traditionally extensively considered in the literature, the recent development of all-dielectric nanophotonics also paves the way to a variety of exciting phenomena based on the manipulation of $|\mathbf{H}|^2$ [89–91], which also can be realized with the multilayered spherical particles of appropriate composition [92]. In any case, a proper understanding of energy density distribution may provide valuable insight in many other situations, some of which are the subject of future investigation.

Corresponding MATLAB routines, which include the theoretical treatment reported in this paper, are presented in Code 1, Ref. [93]. It is straightforward to modify the code to obtain separate contributions for field intensities, and to determine the *stored* and *dissipated* energies for dispersive and absorbing media [54–57] (cf. also Appendix C of Ref. [27]). It is worthwhile to emphasize that a numerical implementation of the developed theory is of low computational cost due to the utilization of explicit analytic expressions for the electromagnetic energy density.

APPENDIX A: VECTOR SPHERICAL HARMONICS

The definition of the vector spherical harmonics from Eq. (2) varies in the literature (compare, for instance, Bohren [7], Jackson [53], Chew [94], and Mishchenko [95]). Here, we provide a "combined" representation for magnetic, longitudinal, and electric vector spherical harmonics in *spherical* (φ, ϑ, r) coordinates:

$$\mathbf{Y}_L^{(m)} = i\sqrt{\frac{(l-m)!}{(l+m)!}}\sqrt{\frac{2l+1}{4\pi l(l+1)}} \times \left[\hat{\mathbf{e}}_\vartheta \frac{im P_l^m(\cos\vartheta)}{\sin\vartheta} - \hat{\mathbf{e}}_\varphi \frac{\mathrm{d}P_l^m(\cos\vartheta)}{\mathrm{d}\vartheta}\right] \exp(im\varphi),$$

$$\mathbf{Y}_L^{(o)} = i\sqrt{\frac{(l-m)!}{(l+m)!}}\sqrt{\frac{2l+1}{4\pi}} P_l^m(\cos\vartheta) \exp(im\varphi)\, \hat{\mathbf{e}}_r,$$

$$\mathbf{Y}_L^{(e)} = i\sqrt{\frac{(l-m)!}{(l+m)!}}\sqrt{\frac{2l+1}{4\pi l(l+1)}} \times \left[\hat{\mathbf{e}}_\vartheta \frac{\mathrm{d}P_l^m(\cos\vartheta)}{\mathrm{d}\vartheta} + \hat{\mathbf{e}}_\varphi \frac{im P_l^m(\cos\vartheta)}{\sin\vartheta}\right] \exp(im\varphi),$$

where $\hat{\mathbf{e}}_\varphi$, $\hat{\mathbf{e}}_\vartheta$, and $\hat{\mathbf{e}}_r$ are corresponding unit vectors, and $P_l^m(x)$ are the associated Legendre functions of the first kind [96] of degree l and order m:

$$P_l^m(x) = \frac{(-1)^m}{2^l l!}(1-x^2)^{m/2}\frac{\mathrm{d}^{l+m}}{\mathrm{d}x^{l+m}}(x^2-1)^l.$$

APPENDIX B: ANGULAR INTEGRATION OF MULTIPOLE FIELDS

Recalling the fact that vector spherical harmonics are orthonormal, i.e.,

$$\oint |\mathbf{Y}_L^{(o,m,e)}(\mathbf{r})|^2 \mathrm{d}\Omega = 1,$$

one obtains for the multipole field $\mathbf{F}_{ML}$ of Eq. (2):

$$\oint |\mathbf{F}_{ML}|^2 \mathrm{d}\Omega = |f_{Ml}(kr)|^2 \oint |\mathbf{Y}_L^{(m)}(\mathbf{r})|^2 \mathrm{d}\Omega = |f_{Ml}(kr)|^2. \tag{B1}$$

After substituting from Eq. (10.1.22) of [96] into Eq. (10.1.20) of [96] in the recurrence relations for the spherical Bessel functions,

$$\frac{(y f_l)'}{y} = f_l' + \frac{f_l}{y} = \frac{l+1}{2l+1} f_{l-1} - \frac{l}{2l+1} f_{l+1}, \tag{B2}$$

and the radial derivative in the multipole field $\mathbf{F}_{EL}$ can be easily eliminated:

$$\mathbf{F}_{EL}(k_n, \mathbf{r}) = \frac{\sqrt{l(l+1)}\, f_{EL}(k_n r)}{k_n r}\mathbf{Y}_L^{(o)}(\mathbf{r}) + \left[\frac{l+1}{2l+1} f_{E,l-1}(k_n r) - \frac{l}{2l+1} f_{E,l+1}(k_n r)\right]\mathbf{Y}_L^{(e)}(\mathbf{r}). \tag{B3}$$

On using the orthonormality of $\mathbf{Y}_L^{(o,m,e)}$, together with Eq. (10.1.19) of [96] applied to the contribution resulting from $\sim \mathbf{Y}_L^{(o)}$ term, Eq. (B3) is transformed into

$$\oint |\mathbf{F}_{EL}|^2 \mathrm{d}\Omega = \frac{l+1}{2l+1}|f_{E,l-1}|^2 + \frac{l}{2l+1}|f_{E,l+1}|^2. \tag{B4}$$

Equations (B1) and (B4) are used to perform angular integration of Eq. (18), which yields in Eq. (19) and Eq. (20).

APPENDIX C: LOMMEL'S INTEGRATION FORMULAS

Consider the defining *spherical* Bessel equation of given order l:

$$\frac{\mathrm{d}^2\mathcal{F}_l(kr)}{\mathrm{d}r^2} + \frac{2}{r}\frac{\mathrm{d}\mathcal{F}_l(kr)}{\mathrm{d}r} + \left[k^2 - \frac{l(l+1)}{r^2}\right]\mathcal{F}_l(kr) = 0, \tag{C1}$$

where r is real in our case, and k is, in general, a complex parameter.

Much the same as in the case of the Lommel formula for the *cylindrical* Bessel equation ([97], Chap. V), the corresponding Lommel formula for two arbitrary solutions $\mathcal{F}_l(\rho r)$ and $\mathcal{G}_l(\sigma r)$ (here, in general, $\sigma \neq \rho$ are arbitrary complex numbers) of the spherical Bessel equation Eq. (C1) with different parameter values follows straightforwardly from the fact that

$$\begin{aligned}\frac{\mathrm{d}}{\mathrm{d}r}&\left[\mathcal{F}_l(\rho r)\frac{\mathrm{d}\mathcal{G}_l(\sigma r)}{\mathrm{d}r} - \frac{\mathrm{d}\mathcal{F}_l(\rho r)}{\mathrm{d}r}\mathcal{G}_l(\sigma r)\right]\\ &= \left[\mathcal{F}_l(\rho r)\frac{\mathrm{d}^2\mathcal{G}_l(\sigma r)}{\mathrm{d}r^2} - \frac{\mathrm{d}^2\mathcal{F}_l(\rho r)}{\mathrm{d}r^2}\mathcal{G}_l(\sigma r)\right]\\ &= -\frac{2}{r}\left[\mathcal{F}_l(\rho r)\frac{\mathrm{d}\mathcal{G}_l(\sigma r)}{\mathrm{d}r} - \frac{\mathrm{d}\mathcal{F}_l(\rho r)}{\mathrm{d}r}\mathcal{G}_l(\sigma r)\right]\\ &\quad + (\rho^2-\sigma^2)\mathcal{F}_l(\rho r)\mathcal{G}_l(\sigma r),\end{aligned}$$

where the latter expression can be recast as

$$\begin{aligned}\frac{\mathrm{d}}{\mathrm{d}r}&\left[r^2\left(\mathcal{F}_l(\rho r)\frac{\mathrm{d}\mathcal{G}_l(\sigma r)}{\mathrm{d}r} - \frac{\mathrm{d}\mathcal{F}_l(\rho r)}{\mathrm{d}r}\mathcal{G}_l(\sigma r)\right)\right]\\ &= r^2\left(\rho^2-\sigma^2\right)\mathcal{F}_l(\rho r)\mathcal{G}_l(\sigma r).\end{aligned}$$

On integrating both sides, one immediately arrives at

$$\begin{aligned}(\rho^2-\sigma^2)&\int^r \mathcal{F}_l(\rho r)\mathcal{G}_l(\sigma r)r^2\mathrm{d}r\\ &= r^2\left[\mathcal{F}_l(\rho r)\frac{\mathrm{d}\mathcal{G}_l(\sigma r)}{\mathrm{d}r} - \frac{\mathrm{d}\mathcal{F}_l(\rho r)}{\mathrm{d}r}\mathcal{G}_l(\sigma r)\right] + \mathcal{C},\end{aligned} \tag{C2}$$

where $\mathcal{C}$ is an integration constant.

In the limit $\rho \to \sigma$, the lhs of Eq. (C2) goes to zero, whereas the rhs seems to be a nonzero function of r. After closer inspection, one finds that the square bracket on the rhs reduces to the Wronskian $W_r\{\mathcal{F}_l(\sigma r), \mathcal{G}_l(\sigma r)\}$. Any solution $\mathcal{F}_l$ and $\mathcal{G}_l$ of Eq. (C1) of order l can be expressed as a linear combination of spherical Bessel functions j_l and n_l with, in general, complex coefficients [cf. Eq. (4)]. Subsequently, the Wronskian $W_r\{\mathcal{F}_l, \mathcal{G}_l\}$ breaks down into a sum of terms proportional to $W_r\{j_l(\sigma r), j_l(\sigma r)\}$, $W_r\{n_l(\sigma r), n_l(\sigma r)\}$, and $W_r\{j_l(\sigma r), n_l(\sigma r)\}$. The first two factors are identically zero. The last one is proportional to $1/r^2$ {Eq. (10.1.6) [96]}, which cancels the factor r^2 in front of the square bracket in Eq. (C2). This means that the term with the square bracket on the rhs of Eq. (C2) reduces to, in general, nonzero constant $\tilde{\mathcal{C}}$ the limit $\rho \to \sigma$. By taking the integration constant $\mathcal{C}$ in Eq. (C2) to be just the opposite of the constant $\tilde{\mathcal{C}}$, both sides of Eq. (C2) go to zero to the limit $\rho \to \sigma$, and the equality is preserved. The point of crucial importance is that for any specific pair of spherical Bessel functions $\mathcal{F}_l$ and $\mathcal{G}_l$, there is a unique constant $\mathcal{C}$, which ensures equality in Eq. (C2) including the limit $\rho \to \sigma$. One can thus readily apply l'Hôpital's rule to investigate the limit $\rho \to \sigma$ of the expression

$$\begin{aligned}\int^r \mathcal{F}_l(\rho r)\mathcal{G}_l(\sigma r)r^2\mathrm{d}r &= \frac{r^2}{\rho^2-\sigma^2}\\ &\times\left[\mathcal{F}_l(\rho r)\frac{\mathrm{d}\mathcal{G}_l(\sigma r)}{\mathrm{d}r} - \frac{\mathrm{d}\mathcal{F}_l(\rho r)}{\mathrm{d}r}\mathcal{G}_l(\sigma r)\right] + \frac{\mathcal{C}}{\rho^2-\sigma^2}.\end{aligned} \tag{C3}$$

Since the constant $\mathcal{C}$ naturally disappears after applying l'Hôpital's rule, or when performing definite integrals, it does not impact final expressions and will be omitted below.

If one wants to consider the special case when $\mathcal{G}_l = \mathcal{F}_l^*$, then, as the result of complex conjugation, also the argument of Bessel functions forming $\mathcal{F}_l$ becomes complex conjugated. An appropriate application of the Lommel's first integral (C3) to this special case is therefore

$$\mathcal{I}_L^{(1)} = \int^r \mathcal{F}_l(\rho r)\mathcal{F}_l^*(\sigma r)r^2 \mathrm{d}r = \frac{r^2}{\rho^2 - \sigma^{*2}}\left[\mathcal{F}_l(\rho r)\frac{\mathrm{d}\mathcal{F}_l^*(\sigma r)}{\mathrm{d}r} - \frac{\mathrm{d}\mathcal{F}_l(\rho r)}{\mathrm{d}r}\mathcal{F}_l^*(\sigma r)\right], \tag{C4}$$

because $\mathcal{F}_l^*(\sigma r)$ satisfies the Bessel equation (C1) with $k = \sigma^*$. After using the recurrence relation for Bessel functions {Eq. (10.1.22) of [96]}

$$\frac{\mathrm{d}\mathcal{F}_l(kr)}{\mathrm{d}r} = \frac{l}{r}\mathcal{F}_l(kr) - k\mathcal{F}_{l+1}(kr),$$

one arrives at

$$\mathcal{I}_L^{(1)} = \frac{r^2}{\rho^2 - \sigma^{*2}}[\rho\mathcal{F}_{l+1}(\rho r)\mathcal{F}_l^*(\sigma r) - \sigma^*\mathcal{F}_l(\rho r)\mathcal{F}_{l+1}^*(\sigma r)].$$

In the special case of $\sigma^* = \rho^*$,

$$\begin{aligned}\int^r \mathcal{F}_l(\rho r)\mathcal{F}_l^*(\rho r)r^2\mathrm{d}r &= \int^r |\mathcal{F}_l(\rho r)|^2 r^2 \mathrm{d}r \\ &= \frac{r^2}{\rho^2 - \rho^{*2}}[\rho\mathcal{F}_{l+1}(\rho r)\mathcal{F}_l^*(\rho r) - \rho^*\mathcal{F}_l(\rho r)\mathcal{F}_{l+1}^*(\rho r)] \\ &= \frac{r^3}{x^2 - x^{*2}}[x\mathcal{F}_{l+1}(x)\mathcal{F}_l^*(x) - x^*\mathcal{F}_l(x)\mathcal{F}_{l+1}^*(x)],\end{aligned} \tag{C5}$$

where $x = \rho r$. The latter expression in square brackets corresponds to our Eq. (31).

In the real limit $\rho^* \to \rho$, which corresponds to a lossless core or a lossless shell in the current work, an application of l'Hôpital's rule and recurrence relations {Eqs. (10.1.21–22) of [96]} for the Bessel functions in Eq. (C5) yields

$$\begin{aligned}\int^r |\mathcal{F}_l(\rho r)|^2 r^2 \mathrm{d}r &= -\frac{r^2}{2\rho}\left[\rho r\mathcal{F}_{l+1}(\rho r)\frac{\mathrm{d}\mathcal{F}_l^*(\rho r)}{\mathrm{d}(\rho r)}\right. \\ &\quad - \rho r\mathcal{F}_l(\rho r)\frac{\mathrm{d}\mathcal{F}_{l+1}^*(\rho r)}{\mathrm{d}(\rho r)} \\ &\quad \left. - \mathcal{F}_l(\rho r)\mathcal{F}_{l+1}^*(\rho r)\right] \\ &= \frac{r^3}{2x}[x(|\mathcal{F}_l(x)|^2 + |\mathcal{F}_{l+1}(x)|^2) \\ &\quad - (2l+1)\mathrm{Re}(\mathcal{F}_l(x)\mathcal{F}_{l+1}^*(x))].\end{aligned}$$

The latter expression in square brackets corresponds to our Eq. (37).

REFERENCES

1. A. L. Aden and M. Kerker, "Scattering of electromagnetic waves from two concentric spheres," J. Appl. Phys. **22**, 1242–1246 (1951).
2. O. B. Toon and T. P. Ackerman, "Algorithms for the calculation of scattering by stratified spheres," Appl. Opt. **20**, 3657–3660 (1981).
3. Z. S. Wu and Y. P. Wang, "Electromagnetic scattering for multilayered sphere: recursive algorithms," Radio Sci. **26**, 1393–1401 (1991).
4. R. Bhandari, "Scattering coefficients for a multilayered sphere: analytic expressions and algorithms," Appl. Opt. **24**, 1960–1967 (1985).
5. D. W. Mackowski, R. A. Altenkirch, and M. P. Menguc, "Internal absorption cross sections in a stratified sphere," Appl. Opt. **29**, 1551–1559 (1990).
6. J. Sinzig and M. Quinten, "Scattering and absorption by spherical multilayer particles," Appl. Phys. A **58**, 157–162 (1994).
7. C. F. Bohren and D. R. Huffman, *Absorption and Scattering of Light by Small Particles* (Wiley-VCH, 1998).
8. W. Yang, "Improved recursive algorithm for light scattering by a multilayered sphere," Appl. Opt. **42**, 1710–1720 (2003).
9. O. Peña and U. Pal, "Scattering of electromagnetic radiation by a multilayered sphere," Comput. Phys. Commun. **180**, 2348–2354 (2009).
10. R. A. Shore, "Scattering of an electromagnetic linearly polarized plane wave by a multilayered sphere: obtaining a computational form of Mie coefficients for the scattered field," IEEE Antennas Propag. Mag. **57**(6), 69–116 (2015).
11. K. Ladutenko, U. Pal, A. Rivera, and O. Peña-Rodríguez, "Mie calculation of electromagnetic near-field for a multilayered sphere," Comput. Phys. Commun. **214**, 225–230 (2017).
12. G. Gouesbet, B. Maheu, and G. Gréhan, "Light scattering from a sphere arbitrarily located in a Gaussian beam, using a Bromwich formulation," J. Opt. Soc. Am. A **5**, 1427–1443 (1988).
13. F. Onofri, G. Gréhan, and G. Gouesbet, "Electromagnetic scattering from a multilayered sphere located in an arbitrary beam," Appl. Opt. **34**, 7113–7124 (1995).
14. Z. S. Wu, L. X. Guo, K. F. Ren, G. Gouesbet, and G. Gréhan, "Improved algorithm for electromagnetic scattering of plane waves and shaped beams by multilayered spheres," Appl. Opt. **36**, 5188–5198 (1997).
15. R. Li, X. Han, L. Shi, K. F. Ren, and H. Jiang, "Debye series for Gaussian beam scattering by a multilayered sphere," Appl. Opt. **46**, 4804–4812 (2007).
16. N. M. Mojarad, G. Zumofen, V. Sandoghdar, and M. Agio, "Metal nanoparticles in strongly confined beams: transmission, reflection and absorption," J. Eur. Opt. Soc. **4**, 09014 (2009).
17. A. E. Neeves and M. H. Birnboim, "Composite structures for the enhancement of nonlinear-optical susceptibility," J. Opt. Soc. Am. B **6**, 787–796 (1989).
18. Y. Pu, R. Grange, C.-L. Hsieh, and D. Psaltis, "Nonlinear optical properties of core-shell nanocavities for enhanced second-harmonic generation," Phys. Rev. Lett. **104**, 207402 (2010).
19. J. Butet, I. Russier-Antoine, C. Jonin, N. Lascoux, E. Benichou, and P.-F. Brevet, "Nonlinear Mie theory for the second harmonic generation in metallic nanoshells," J. Opt. Soc. Am. B **29**, 2213–2221 (2012).
20. J. A. Gordon and R. W. Ziolkowski, "The design and simulated performance of a coated nano-particle laser," Opt. Express **15**, 2622–2653 (2007).
21. M. A. Noginov, G. Zhu, A. M. Belgrave, R. Bakker, V. M. Shalaev, E. E. Narimanov, S. Stout, E. Herz, T. Suteewong, and U. Wiesner, "Demonstration of a spaser-based nanolaser," Nature **460**, 1110–1112 (2009).
22. N. Passarelli, R. A. Bustos-Marún, and E. A. Coronado, "Spaser and optical amplification conditions in gold-coated active nanoparticles," J. Phys. Chem. C **120**, 24941–24949 (2016).
23. N. Harris, M. J. Ford, and M. B. Cortie, "Optimization of plasmonic heating by gold nanospheres and nanoshells," J. Phys. Chem. B **110**, 10701–10707 (2006).
24. B. S. Luk'yanchuk, A. E. Miroshnichenko, M. I. Tribelsky, Y. S. Kivshar, and A. R. Khokhlov, "Paradoxes in laser heating of plasmonic nanoparticles," New J. Phys. **14**, 093022 (2012).

25. O. Neumann, A. S. Urban, J. Day, S. Lal, P. Nordlander, and N. J. Halas, "Solar vapor generation enabled by nanoparticles," ACS Nano **7**, 42–49 (2013).
26. A. E. Schlather, A. Manjavacas, A. Lauchner, V. S. Marangoni, C. J. DeSantis, P. Nordlander, and N. J. Halas, "Hot hole photoelectrochemistry on Au@SiO2@Au nanoparticles," J. Phys. Chem. Lett. **8**, 2060–2067 (2017).
27. A. Moroz, "A recursive transfer-matrix solution for a dipole radiating inside and outside a stratified sphere," Ann. Phys. (N.Y.) **315**, 352–418 (2005).
28. A. Moroz, "Spectroscopic properties of a two-level atom interacting with a complex spherical nanoshell," Chem. Phys. **317**, 1–15 (2005).
29. C. Ayala-Orozco, J. G. Liu, M. W. Knight, Y. Wang, J. K. Day, P. Nordlander, and N. J. Halas, "Fluorescence enhancement of molecules inside a gold nanomatryoshka," Nano Lett. **14**, 2926–2933 (2014).
30. N. Sakamoto, T. Onodera, T. Dezawa, Y. Shibata, and H. Oikawa, "Highly enhanced emission of visible light from core-dual-shell-type hybridized nanoparticles," Part. Part. Syst. Charact. **34**, 1700258 (2017).
31. D. M. Wu, A. García-Etxarri, A. Salleo, and J. A. Dionne, "Plasmon-enhanced upconversion," J. Phys. Chem. Lett. **5**, 4020–4031 (2014).
32. I. L. Rasskazov, L. Wang, C. J. Murphy, R. Bhargava, and P. S. Carney, "Plasmon-enhanced upconversion: engineering enhancement and quenching at nano and macro scales," Opt. Mater. Express **8**, 3787–3804 (2018).
33. G. D. Moon, J. B. Joo, M. Dahl, H. Jung, and Y. Yin, "Nitridation and layered assembly of hollow TiO2 shells for electrochemical energy storage," Adv. Funct. Mater. **24**, 848–856 (2014).
34. L. Meng, R. Yu, M. Qiu, and F. J. García de Abajo, "Plasmonic nano-oven by concatenation of multishell photothermal enhancement," ACS Nano **11**, 7915–7924 (2017).
35. A. D. Phan, N. B. Le, N. T. H. Lien, and K. Wakabayashi, "Multilayered plasmonic nanostructures for solar energy harvesting," J. Phys. Chem. C **122**, 19801–19806 (2018).
36. W. Li, A. Elzatahry, D. Aldhayan, and D. Zhao, "Core-shell structured titanium dioxide nanomaterials for solar energy utilization," Chem. Soc. Rev. **47**, 8203–8237 (2018).
37. A. K. Kodali, X. Llora, and R. Bhargava, "Optimally designed nanolayered metal-dielectric particles as probes for massively multiplexed and ultrasensitive molecular assays," Proc. Natl. Acad. Sci. USA **107**, 13620–13625 (2010).
38. O. Peña-Rodríguez and U. Pal, "Enhanced plasmonic behavior of bimetallic (Ag-Au) multilayered spheres," Nanoscale Res. Lett. **6**, 279 (2011).
39. N. G. Khlebtsov and B. N. Khlebtsov, "Optimal design of gold nanomatryoshkas with embedded Raman reporters," J. Quant. Spectrosc. Radiat. Transfer **190**, 89–102 (2017).
40. P. K. Jain, K. S. Lee, I. H. El-Sayed, and M. A. El-Sayed, "Calculated absorption and scattering properties of gold nanoparticles of different size, shape, and composition: applications in biological imaging and biomedicine," J. Phys. Chem. B **110**, 7238–7248 (2006).
41. B. N. Khlebtsov and N. G. Khlebtsov, "Biosensing potential of silica/gold nanoshells: sensitivity of plasmon resonance to the local dielectric environment," J. Quant. Spectrosc. Radiat. Transfer **106**, 154–169 (2007).
42. R. Ghosh Chaudhuri and S. Paria, "Core/shell nanoparticles: classes, properties, synthesis mechanisms, characterization, and applications," Chem. Rev. **112**, 2373–2433 (2012).
43. C. Ayala-Orozco, C. Urban, M. W. Knight, A. S. Urban, O. Neumann, S. W. Bishnoi, S. Mukherjee, A. M. Goodman, H. Charron, T. Mitchell, M. Shea, R. Roy, S. Nanda, R. Schiff, N. J. Halas, and A. Joshi, "Au nanomatryoshkas as efficient near-infrared photothermal transducers for cancer treatment: benchmarking against nanoshells," ACS Nano **8**, 6372–6381 (2014).
44. V. I. Zakomirnyi, I. L. Rasskazov, S. V. Karpov, and S. P. Polyutov, "New ideally absorbing Au plasmonic nanostructures for biomedical applications," J. Quant. Spectrosc. Radiat. Transfer **187**, 54–61 (2017).
45. B. J. Messinger, K. U. von Raben, R. K. Chang, and P. W. Barber, "Local fields at the surface of noble-metal microspheres," Phys. Rev. B **24**, 649–657 (1981).
46. A. Bott and W. Zdunkowski, "Electromagnetic energy within dielectric spheres," J. Opt. Soc. Am. A **4**, 1361–1365 (1987).
47. T. J. Arruda and A. S. Martinez, "Electromagnetic energy within magnetic spheres," J. Opt. Soc. Am. A **27**, 992–1001 (2010).
48. T. J. Arruda, F. A. Pinheiro, and A. S. Martinez, "Electromagnetic energy within single-resonance chiral metamaterial spheres," J. Opt. Soc. Am. A **30**, 1205–1212 (2013).
49. T. J. Arruda, F. A. Pinheiro, and A. S. Martinez, "Electromagnetic energy within coated spheres containing dispersive metamaterials," J. Opt. **14**, 065101 (2012).
50. W. H. Peirce, "Numerical integration over the spherical shell," Math. Computation **11**, 244 (1957).
51. D. E. Goldberg, *Genetic Algorithms in Search, Optimization and Machine Learning* (Addison-Wesley, 1989).
52. R. Storn and K. Price, "Differential evolution—a simple and efficient heuristic for global optimization over continuous spaces," J. Global Optim. **11**, 341–359 (1997).
53. J. D. Jackson, *Classical Electrodynamics*, 3rd ed. (Wiley, 1999).
54. R. Loudon, "The propagation of electromagnetic energy through an absorbing dielectric," J. Phys. A **3**, 233–245 (1970).
55. R. Ruppin, "Electromagnetic energy in dispersive spheres," J. Opt. Soc. Am. A **15**, 524–527 (1998).
56. R. Ruppin, "Electromagnetic energy density in a dispersive and absorptive material," Phys. Lett. A **299**, 309–312 (2002).
57. F. D. Nunes, T. C. Vasconcelos, M. Bezerra, and J. Weiner, "Electromagnetic energy density in dispersive and dissipative media," J. Opt. Soc. Am. B **28**, 1544–1552 (2011).
58. M. I. Mishchenko, "Light scattering by randomly oriented axially symmetric particles," J. Opt. Soc. Am. A **8**, 871–882 (1991).
59. J. D. Pendleton, "Sum rules for products of light scattering functions," J. Opt. Soc. Am. A **18**, 610–613 (2001).
60. H. Xu, "Multilayered metal core-shell nanostructures for inducing a large and tunable local optical field," Phys. Rev. B **72**, 073405 (2005).
61. A. E. Miroshnichenko, "Off-resonance field enhancement by spherical nanoshells," Phys. Rev. A **81**, 053818 (2010).
62. T. J. Arruda, A. S. Martinez, and F. A. Pinheiro, "Unconventional Fano effect and off-resonance field enhancement in plasmonic coated spheres," Phys. Rev. A **87**, 043841 (2013).
63. W. J. Wiscombe, "Improved Mie scattering algorithms," Appl. Opt. **19**, 1505–1509 (1980).
64. J. R. Allardice and E. C. Le Ru, "Convergence of Mie theory series: criteria for far-field and near-field properties," Appl. Opt. **53**, 7224–7229 (2014).
65. H. S. Zhou, I. Honma, H. Komiyama, and J. W. Haus, "Controlled synthesis and quantum-size effect in gold-coated nanoparticles," Phys. Rev. B **50**, 12052–12056 (1994).
66. C. Graf and A. van Blaaderen, "Metallodielectric colloidal core-shell particles for photonic applications," Langmuir **18**, 524–534 (2002).
67. K. Hasegawa, C. Rohde, and M. Deutsch, "Enhanced surface-plasmon resonance absorption in metal-dielectric-metal layered microspheres," Opt. Lett. **31**, 1136–1138 (2006).
68. V. Grigoriev, N. Bonod, J. Wenger, and B. Stout, "Optimizing nanoparticle designs for ideal absorption of light," ACS Photon. **2**, 263–270 (2015).
69. K. Ladutenko, P. Belov, O. Peña-Rodríguez, A. Mirzaei, A. E. Miroshnichenko, and I. V. Shadrivov, "Superabsorption of light by nanoparticles," Nanoscale **7**, 18897–18901 (2015).
70. Z. Ruan and S. Fan, "Design of subwavelength superscattering nanospheres," Appl. Phys. Lett. **98**, 043101 (2011).
71. C. Rohde, K. Hasegawa, and M. Deutsch, "Plasmon-assisted transparency in metal-dielectric microspheres," Opt. Lett. **32**, 415–417 (2007).
72. A. Alù and N. Engheta, "Multifrequency optical invisibility cloak with layered plasmonic shells," Phys. Rev. Lett. **100**, 113901 (2008).
73. N. J. Hudak, B. S. Garrett, B. G. DeLacy, and M. S. Mirotznik, "Iterative design of multilayered dielectric microspheres with tunable transparency windows," J. Opt. Soc. Am. A **36**, 705–715 (2019).

74. A. Moroz and C. Sommers, "Photonic band gaps of three-dimensional face-centred cubic lattices," J. Phys. Condens. Matter **11**, 997–1008 (1999).
75. A. Moroz, "Photonic crystals of coated metallic spheres," Europhys. Lett. **50**, 466–472 (2000).
76. A. Moroz, "Metallo-dielectric diamond and zinc-blende photonic crystals," Phys. Rev. B **66**, 115109 (2002).
77. D. D. Smith and K. A. Fuller, "Photonic bandgaps in Mie scattering by concentrically stratified spheres," J. Opt. Soc. Am. B **19**, 2449–2455 (2002).
78. P. Wang, A. V. Krasavin, F. N. Viscomi, A. M. Adawi, J.-S. G. Bouillard, L. Zhang, D. J. Roth, L. Tong, and A. V. Zayats, "Metaparticles: dressing nano-objects with a hyperbolic coating," Laser Photon. Rev. **12**, 1800179 (2018).
79. P. B. Johnson and R. W. Christy, "Optical constants of the noble metals," Phys. Rev. B **6**, 4370–4379 (1972).
80. A. Moroz, "Electron mean free path in a spherical shell geometry," J. Phys. Chem. C **112**, 10641–10652 (2008).
81. R. Ruppin, "Nanoshells with a gain layer: the effects of surface scattering," J. Opt. **17**, 125004 (2015).
82. M. G. Blaber, M. D. Arnold, and M. J. Ford, "Search for the ideal plasmonic nanoshell: the effects of surface scattering and alternatives to gold and silver," J. Phys. Chem. C **113**, 3041–3045 (2009).
83. F. Frezza, F. Mangini, and N. Tedeschi, "Electromagnetic scattering by two concentric spheres buried in a stratified material," J. Opt. Soc. Am. A **32**, 277 (2015).
84. F. Frezza and F. Mangini, "Electromagnetic scattering of an inhomogeneous elliptically polarized plane wave by a multilayered sphere," J. Electromagn. Waves **30**, 492–504 (2016).
85. W. L. Moreira, A. A. R. Neves, M. K. Garbos, T. G. Euser, and C. L. Cesar, "Expansion of arbitrary electromagnetic fields in terms of vector spherical wave functions," Opt. Express **24**, 2370–2382 (2016).
86. Y.-L. Geng, X.-B. Wu, L.-W. Li, and B.-R. Guan, "Electromagnetic scattering by an inhomogeneous plasma anisotropic sphere of multilayers," IEEE Trans. Antennas Propag. **53**, 3982–3989 (2005).
87. C.-W. Qiu, S. Zouhdi, and A. Razek, "Modified spherical wave functions with anisotropy ratio: application to the analysis of scattering by multilayered anisotropic shells," IEEE Trans. Antennas Propag. **55**, 3515–3523 (2007).
88. T. Kaiser, S. Lange, and G. Schweiger, "Structural resonances in a coated sphere: investigation of the volume-averaged source function and resonance positions," Appl. Opt. **33**, 7789–7797 (1994).
89. D. G. Baranov, R. S. Savelev, S. V. Li, A. E. Krasnok, and A. Alù, "Modifying magnetic dipole spontaneous emission with nanophotonic structures," Laser Photon. Rev. **11**, 1600268 (2017).
90. J. Li, N. Verellen, and P. Van Dorpe, "Enhancing magnetic dipole emission by a nano-doughnut-shaped silicon disk," ACS Photon. **4**, 1893–1898 (2017).
91. P. R. Wiecha, C. Majorel, C. Girard, A. Arbouet, B. Masenelli, O. Boisron, A. Lecestre, G. Larrieu, V. Paillard, and A. Cuche, "Enhancement of electric and magnetic dipole transition of rare-earth-doped thin films tailored by high-index dielectric nanostructures," Appl. Opt. **58**, 1682–1690 (2019).
92. D. Tzarouchis and A. Sihvola, "Light scattering by a dielectric sphere: perspectives on the Mie resonances," Appl. Sci. **8**, 184 (2018).
93. I. L. Rasskazov, "STRATIFY GitLab," 2019, https://gitlab.com/iliarasskazov/stratify.
94. M. Kerker, D.-S. Wang, and H. Chew, "Surface enhanced Raman scattering (SERS) by molecules adsorbed at spherical particles," Appl. Opt. **19**, 3373–3388 (1980).
95. M. I. Mishchenko, L. D. Travis, and A. A. Lacis, *Scattering, Absorption, and Emission of Light by Small Particles* (Cambridge University, 2002).
96. M. Abramowitz and I. A. Stegun, *Handbook of Mathematical Functions* (Dover, 1973).
97. G. N. Watson, *A Treatise on the Theory of Bessel Functions*, Cambridge Mathematical Library (Cambridge University, 1995).